# Spin-Down of Radio Millisecond Pulsars at Genesis

Thomas M. Tauris

*Science* **335**, 561 (2012);
DOI: 10.1126/science.1216355

7. E. L. Sikes, C. R. Samson, T. P. Guilderson, W. R. Howard, *Nature* **405**, 555 (2000).
8. L. C. Skinner, S. Fallon, C. Waelbroeck, E. Michel, S. Barker, *Science* **328**, 1147 (2010).
9. A. L. Magana *et al.*, *Paleoceanography* **115**, PA4102 (2010).
10. T.-H. Peng, W. S. Broecker, *Nucl. Instrum. Methods Phys. Res. B* **5**, 346 (1984).
11. S. P. Bryan, T. M. Marchitto, S. J. Lehman, *Earth Planet. Sci. Lett.* **298**, 244 (2010).
12. T. M. Marchitto, S. J. Lehman, J. D. Ortiz, J. Flückiger, A. van Geen, *Science* **316**, 1456 (2007).
13. D. J. R. Thornalley, S. Barker, W. S. Broecker, H. Elderfield, I. N. McCave, *Science* **331**, 202 (2011).
14. A. Burke *et al.*, *Deep Sea Res. Part I Oceanogr. Res. Pap.* **57**, 1510 (2010).
15. R. G. Waller, K. M. Scanlon, L. F. Robinson, *PLoS ONE* **6**, e16153 (2011).
16. Materials and methods are available as supporting material on *Science* Online.
17. $^{14}C$ is a measure of the relative difference between the radiocarbon activity of an absolute international standard and that of a sample, after correction for both age and $^{13}C$.
18. M. Stuiver, H. Polach, *Radiocarbon* **19**, 355 (1977).
19. R. M. Key *et al.*, *Global Biogeochem. Cycles* **18**, GB4031 (2004).
20. B. B. Stephens, R. F. Keeling, *Nature* **404**, 171 (2000).
21. M. Butzin, M. Prange, G. Lohmann, *Earth Planet. Sci. Lett.* **235**, 45 (2005).
22. A. Schmittner, *Earth Planet. Sci. Lett.* **213**, 53 (2003).
23. H. Fischer *et al.*, *Earth Planet. Sci. Lett.* **260**, 340 (2007).
24. R. Francois *et al.*, *Nature* **389**, 929 (1997).
25. D. C. Lund, J. F. Adkins, R. Ferrari, *Paleoceanography* **26**, PA1213 (2011).
26. D. M. Sigman, M. P. Hain, G. H. Haug, *Nature* **466**, 47 (2010).
27. S. Barker, G. Knorr, M. J. Vautravers, P. Diz, L. C. Skinner, *Nat. Geosci.* **3**, 567 (2010).
28. R. De Pol-Holz, L. Keigwin, J. Southon, D. Hebbeln, M. Mohtadi, *Nat. Geosci.* **3**, 192 (2010).
29. J. Ahn, E. J. Brook, *Science* **322**, 83 (2008).
30. L. C. Skinner, N. J. Shackleton, *Paleoceanography* **19**, PA2005 (2004).
31. A. Mangini *et al.*, *Earth Planet. Sci. Lett.* **293**, 269 (2010).
32. M. P. Hain, D. M. Sigman, G. H. Haug, *Geophys. Res. Lett.* **38**, L04604 (2011).
33. C. Laj *et al.*, *Earth Planet. Sci. Lett.* **200**, 177 (2002).
34. M. Frank *et al.*, *Earth Planet. Sci. Lett.* **149**, 121 (1997).
35. R. Muscheler *et al.*, *Earth Planet. Sci. Lett.* **219**, 325 (2004).
36. G. H. Denton, W. S. Broecker, R. B. Alley, *Pages News* **14**, 14 (2006).
37. W. Broecker *et al.*, *Paleoceanography* **22**, PA2206 (2007).
38. A. H. Orsi, T. Whitworth III, W. D. Nowlin Jr., *Deep Sea Res. Part I Oceanogr. Res. Pap.* **42**, 641 (1995).
39. S. J. Goldstein, D. W. Lea, S. Chakraborty, M. Kashgarian, M. T. Murrell, *Earth Planet. Sci. Lett.* **193**, 167 (2001).
40. L. F. Robinson, T. van de Flierdt, *Geology* **37**, 195 (2009).
41. B. Lemieux-Dudon *et al.*, *Quat. Sci. Rev.* **29**, 8 (2010).
42. J. R. Petit *et al.*, *Nature* **399**, 429 (1999).
43. C. Barbante *et al.*; EPICA Community Members, *Nature* **444**, 195 (2006).



**Acknowledgments:** This research was funded by NSF grants 0636787, 0944474, 0902957, 0338087, and 0819714. The data reported in this study are tabulated in the supporting online material. We acknowledge R. Waller and the science parties of cruises LMG06-05 and NBP08-05 for supplying samples used in this study. We also thank the crews of the R/V *Nathaniel B. Palmer* and R/V *Laurence M. Gould*, NOSAMS staff, the WHOI plasma facility, J. Blusztajn, M. Auro, and two anonymous reviewers for help with this project.


**Supporting Online Material**

www.sciencemag.org/cgi/content/full/science.1208163/DC1
Materials and Methods
Figs. S1 to S5
Tables S1 to S3
References (*44*–*56*)


10 May 2011; accepted 30 November 2011
Published online 15 December 2011;
10.1126/science.1208163




# Spin-Down of Radio Millisecond Pulsars at Genesis


**Thomas M. Tauris**



**Millisecond pulsars are old neutron stars that have been spun up to high rotational frequencies via accretion of mass from a binary companion star. An important issue for understanding the physics of the early spin evolution of millisecond pulsars is the impact of the expanding magnetosphere during the terminal stages of the mass-transfer process. Here, I report binary stellar evolution calculations that show that the braking torque acting on a neutron star, when the companion star decouples from its Roche lobe, is able to dissipate >50% of the rotational energy of the pulsar. This effect may explain the apparent difference in observed spin distributions between x-ray and radio millisecond pulsars and help account for the noticeable age discrepancy with their young white dwarf companions.**


Millisecond pulsars (MSPs) are rapidly spinning, strongly magnetized neutron stars. They form as the result of stellar cannibalism, where matter and angular momentum flow from a donor star to an accreting neutron star (*1*, *2*). During this process the system is detectable as an x-ray source (*3*). In some cases, x-ray pulsations reveal a fast spinning neutron star (*4*); the 13 known accreting x-ray MSPs (AXMSPs) have an average spin period of $\langle P \rangle_{\rm AXMSP} = 3.3$ ms (*5*). These AXMSPs are thought to be the evolutionary progenitors of radio MSPs. When the donor star decouples from its Roche lobe (*6*) and the mass transfer generating the x-rays ceases, the radio emission is activated (*7*). Until now more than 200 recycled radio MSPs have been detected in our galaxy, both in the field and in globular clusters, with spin periods between 1.4 and 20 ms. These MSPs, which are observed after the Roche-lobe decoupling phase (RLDP), have $\langle P \rangle_{\rm MSP} = 5.5$ ms (*5*) [see (*8*) for a critical discussion on selection effects and statistics]. It is unknown whether this spin difference is caused by the role of the RLDP or subsequent spin-down from magnetodipole radiation during the lifetime of the radio MSPs.

The interplay between the magnetic field of a neutron star and the conducting plasma of the accreted material is known to provide the accretion torque necessary to spin up the pulsar (*9*–*11*). However, these interactions can also lead to a torque reversal under certain conditions (*12*), especially when the mass-transfer rate decreases (*13*). Similarly, detailed studies of low-mass x-ray binaries (LMXBs) using stellar evolution codes have demonstrated (*14*–*17*) that these systems undergo a long, stable phase of mass transfer, which provides sufficient mass to spin up the accreting neutron star to spin periods of milliseconds. However, these previous studies did not combine such numerical stellar evolution calculations with computations of the resulting accretion torque at work. Here, I compute this torque during the termination of the mass-transfer phase by integrating these two methods, using the time-dependent mass-transfer rate to follow its effect on the pulsar spin rate.

The computation of an LMXB donor star detaching from its Roche lobe is shown in Fig. 1 [see further details in (*8*)]. The full length of the mass-transfer phase was about 1 billion years (Gy); the RLDP happened in the past 200 million years (My) when the mass-transfer rate decreased rapidly. The original mass of the donor star was 1.0 $M_\odot$, and by the time it entered the final stage of the RLDP it had lost 99% of its envelope mass, encapsulating a core of 0.24 $M_\odot$ (i.e., the mass of the hot white dwarf being formed after the RLDP). The orbital period at this stage was 5.1 days, and the MSP had a mass of 1.53 $M_\odot$. By using the received mass-transfer rate, $\dot{M}(t)$, from my stellar models, the radius of the magnetospheric boundary of the pulsar, located at the inner edge of the accretion disk, can be written as $r_{\rm mag} = \varphi \cdot r_{\rm A}$ [with $r_{\rm A}$, the Alfvén radius (*18*), calculated (*8*) following standard prescriptions in the literature (*11*, *19*)]. Knowledge of the relative location of $r_{\rm mag}$, the corotation radius, $r_{\rm co}$, and the light cylinder radius, $r_{\rm lc}$, enabled a computation of the accretion torque acting on the pulsar (*8*) (fig. S1). After a long phase of mass transfer as an LMXB, the pulsar was spinning at its equilibrium period when entering the RLDP. The rapid torque reversals (unresolved in the center panel of Fig. 1; see also fig. S1) originated from successive, small episodes of spin-up or spin-down depending on the relative location of $r_{\rm co}$ and $r_{\rm mag}$, which reflects the small fluctuations in $\dot{M}(t)$. However, this equilibrium was broken when $\dot{M}(t)$ decreased substantially on a short time scale. That resulted in $r_{\rm mag}$ increasing on a time scale ($t_{\rm RLDP}$) faster than the spin-relaxation


Argelander-Institut für Astronomie, Universität Bonn, Auf dem Hügel 71, 53121 Bonn, Germany. Max-Planck-Institut für Radioastronomie, Auf dem Hügel 69, 53121 Bonn, Germany. E-mail: tauris@astro.uni-bonn.de

time scale, $t_{torque}$, on which the torque would transmit the effect of deceleration to the neutron star, and therefore $r_{mag} > r_{co}$. In this propeller phase (*12*), a centrifugal barrier arose and expelled material entering the magnetosphere, whereby a braking torque acted to slow down the spin rate of the pulsar even further (see bottom panel in Fig. 1 and fig. S2). The spin-relaxation time scale is given by $t_{torque} \simeq J/N$, which yields:

$$t_{torque} \simeq 50\ \mathrm{My} \cdot B_8^{-8/7} \left(\frac{\dot{M}}{0.1\dot{M}_{Edd}}\right)^{-3/7} \left(\frac{M}{1.4M_\odot}\right)^{17/7} \quad (1)$$

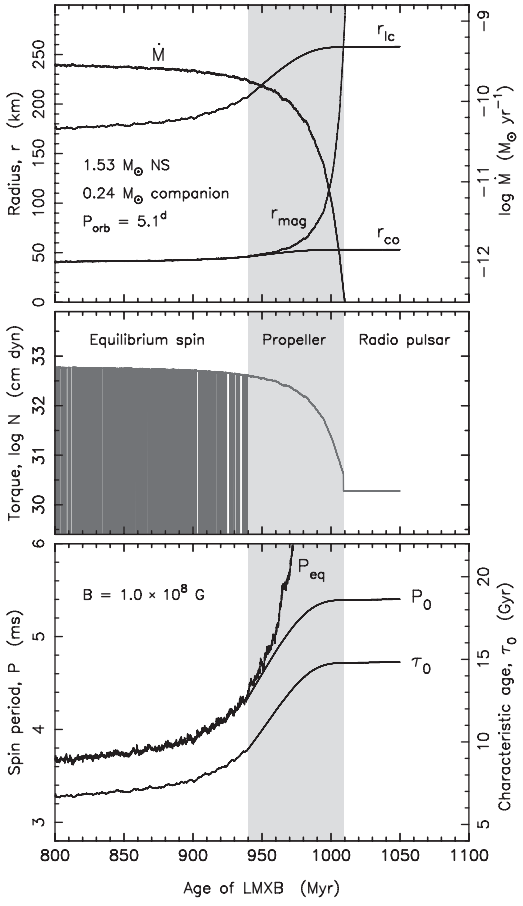


**Fig. 1.** Final stages of mass transfer in an LMXB. The gradual decoupling of the donor star from its Roche lobe causes the received mass-transfer rate, $\dot{M}$ (i.e., the ram pressure of the inflowing material), to decrease, whereby the magnetospheric boundary of the neutron star, $r_{mag}$, moves outward relative to the corotation radius, $r_{co}$, and the light cylinder radius, $r_{lc}$ (**top**). The alternating spin-up/spin-down torques during the equilibrium spin phase are replaced by a continuous spin-down torque in the propeller phase ($r_{co} < r_{mag} < r_{lc}$), until the pulsar activates its radio emission and the magnetodipole radiation remains as the sole braking mechanism [**center**; see also (*8*) and figs. S1 and S2]. After an initial phase of spin-down, the spin equilibrium is broken, which limits the loss of rotational energy of the pulsar and sets the value of the spin period, $P_0$, of the radio MSP at birth (**bottom**). Also shown in the bottom panel is the resulting characteristic age, $\tau_0 \propto P_0^2$, of the recycled radio MSP, assuming a constant B field of $10^8$ G during the RLDP. The gray shaded regions indicate the propeller phase.

where the spin angular momentum of the neutron star is $J = 2\pi I/P$ and the braking torque at the magnetospheric boundary is roughly given by $N \sim \dot{M}\sqrt{GMr_{mag}}$ (*8*). Here, $G$ is the gravitational constant; $M$ and $I$ are the neutron star mass and moment of inertia, respectively; and $B_8$ is the surface magnetic flux density in units of $10^8$ G. In addition to this torque, the magnetic field drag on the disk (*20*) was included in the model, although this effect is usually less dominant. In these calculations, I assumed that the strength of the neutron star B field has reached a constant, residual level before the propeller phase, a reasonable assumption given that less than 1% of the donor star envelope mass remained to be transferred. The propeller phase was terminated when $r_{mag} > r_{lc}$. At this point, the MSP activated its radio emission and turned on a plasma wind, which then inhibited any further accretion onto the neutron star (*13*, *21*). The duration of the RLDP in this example was $t_{RLDP} > 100$ My (including early stages before the propeller phase), which is a substantial fraction of the spin-relaxation time scale, $t_{torque} \approx 200$ My, calculated by using Eq. 1 at the onset of the propeller phase. For this reason, the RLDP has an important effect on the spin rate, $P_0$, and the characteristic age of the radio MSP at birth, $\tau_0$. In the case reported here, the radio MSP was born (recycled) with $P_0 \approx 5.4$ ms and an initial so-called characteristic age $\tau_0 \equiv P_0/2\dot{P}_0 \approx 15$ Gy. The spin period before the RLDP was about 3.7 ms, implying that this MSP lost more than 50% of its rotational energy during the RLDP. If the pulsar had not broken its spin equilibrium during the RLDP, it would have been recycled with a slow spin period of $P_0 \approx 58$ ms and thus not become an MSP (*22*).

Radio pulsars emit magnetic dipole radiation as well as a plasma wind (*19*, *23*). These effects cause rotational energy to be lost, and hence radio MSPs

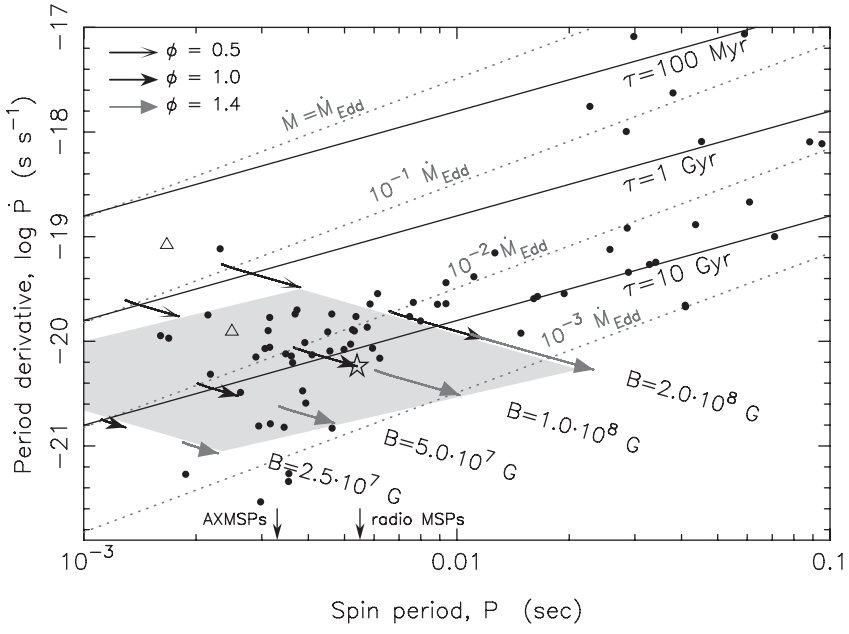


**Fig. 2.** Evolutionary tracks during the RLDP. Computed tracks are shown as arrows in the $P\dot{P}$ diagram, calculated by using different values of the neutron star B-field strength. The various types of arrows correspond to different values of the magnetospheric coupling parameter, φ. The gray-shaded area indicates all possible birth locations of recycled MSPs calculated from one donor star model. The solid lines represent characteristic ages, τ, and the dotted lines are spin-up lines calculated for a magnetic inclination angle, $\alpha = 90°$. The star indicates the radio MSP birth location for the case presented in Fig. 1. The two triangles indicate approximate locations (*36*) of the AXMSPs SWIFT J1756.9−2508 (upper) and SAX 1808.4−3658 (lower). Observed MSPs in the Galactic field are shown as dots [data taken from the *ATNF Pulsar Catalogue*, December 2011]. All the measured $\dot{P}$ values are corrected for the Shklovskii effect, a kinematic projection effect that affects the apparent value of $\dot{P}$ for pulsars (*37*). If the transverse velocity of a given pulsar was unknown, I used a value of 72 km $s^{-1}$, the median value of the 44 measured MSP velocities. The average spin periods of AXMSPs and radio MSPs are indicated with arrows at the bottom of the diagram (*8*).

will slow down their spin rates with time after the RLDP. However, they cannot explain the apparent difference in spin distributions between AXMSPs and radio MSPs, because radio MSPs, which have weak surface magnetic field strengths, could not spin down by the required amount even in a Hubble time. The true age of a pulsar (*23*) is given by $t = P/((n-1)\dot{P})[1-(P_0/P)^{n-1}]$. Assuming an evolution with a braking index $n = 3$ and $B = 1.0\times 10^8$ G, the time scale $t$ is larger than 10 Gy, using $P_0 = \langle P\rangle_{\mathrm{AXMSP}} = 3.3$ ms and $P(t) = \langle P\rangle_{\mathrm{MSP}} = 5.5$ ms. To make things worse, one has to add the main-sequence lifetime of the LMXB donor star, which is typically 3 to 12 Gy, thereby reaching unrealistic large total ages. Although the statistics of AXMSPs still has its basis in small numbers and care must be taken for both detection biases (such as eclipsing effects of radio MSPs) and comparison between various subpopulations (*8*), it is evident from both observations and theoretical work that the RLDP effect presented here plays an important role for the spin distribution of MSPs.

The RLDP effect may also help explain a few other puzzles, for example, why characteristic (or spin-down) ages of radio MSPs often largely exceed cooling age determinations of their white dwarf companions (*24*). It has been suggested that standard cooling models of white dwarfs may not be correct (*25*–*27*), particularly for low-mass helium white dwarfs. These white dwarfs avoid hydrogen shell flashes at early stages and retain thick hydrogen envelopes, at the bottom of which residual hydrogen burning can continue for several billion years after their formation, keeping the white dwarfs relatively hot (~$10^4$ K) and thereby appearing much younger than they actually are. However, it is well known that the characteristic age is not a trustworthy measure of true age (*28*), and the RLDP effect exacerbates this discrepancy even further. In the model calculation presented in Fig. 1, it was assumed that $B = 1.0\times 10^8$ G and $\varphi = 1.0$. However, $P_0$ and $\tau_0$ depend strongly on both $B$ and $\varphi$. This is shown in Fig. 2, where I have calculated the RLDP effect for different choices of $B$ and $\varphi$ by using the same stellar donor model [i.e., same $\dot{M}(t)$ profile] as before. The use of other LMXB donor star masses, metallicities, and initial orbital periods would lead to other $\dot{M}(t)$ profiles (*16*, *17*) and hence different evolutionary tracks. The conclusion is that recycled MSPs can basically be born with any characteristic age. Thus, we are left with the cooling age of the white dwarf companion as the sole reliable, although still not accurate, measure as an age indicator.

A final puzzle is why no sub-millisecond pulsars have been found among the 216 radio MSPs detected in total so far. Although modern observational techniques are sensitive enough to pick up sub-millisecond radio pulsations, the fastest spinning known radio MSP, J1748−2446ad (*29*), has a spin frequency of only 716 Hz, corresponding to a spin period of 1.4 ms. This spin rate is far from the expected minimum equilibrium spin period (*8*) and the physical mass shedding limit of about 1500 Hz. It has been suggested that gravitational wave radiation during the accretion phase halts the spin period above a certain level (*30*, *31*). The RLDP effect presented here is a promising candidate for an alternative mechanism, in case a sub-millisecond AXMSP is detected (*8*).

### References and Notes


1. M. A. Alpar, A. F. Cheng, M. A. Ruderman, J. Shaham, *Nature* **300**, 728 (1982).
2. D. Bhattacharya, E. P. J. van den Heuvel, *Phys. Rep.* **203**, 1 (1991).
3. L. Bildsten *et al.*, *Astrophys. J. Suppl. Ser.* **113**, 367 (1997).
4. R. Wijnands, M. van der Klis, *Nature* **394**, 344 (1998).
5. J. W. T. Hessels *et al.*, *AIP Conf. Proc.* **1068**, 130 (2008).
6. The Roche lobe of a binary star is the innermost equipotential surface passing through the first Lagrangian point, L1. If a star fills its Roche lobe, the unbalanced pressure at L1 will cause mass transfer to the other star (*2*).
7. A. M. Archibald *et al.*, *Science* **324**, 1411 (2009); 10.1126/science.1172740.
8. Materials and methods are available as supporting material on *Science* Online.
9. F. K. Lamb, C. J. Pethick, D. A. Pines, *Astrophys. J.* **184**, 271 (1973).
10. P. Ghosh, F. K. Lamb, *NATO Sci. Ser.* **377**, 487 (1992).
11. J. Frank, A. King, D. J. Raine, *Accretion Power in Astrophysics* (Cambridge Univ. Press, Cambridge, 2002).
12. A. F. Illarionov, R. A. Sunyaev, *Astron. Astrophys.* **39**, 185 (1975).
13. M. Ruderman, J. Shaham, M. Tavani, *Astrophys. J.* **336**, 507 (1989).
14. R. F. Webbink, S. Rappaport, G. J. Savonije, *Astrophys. J.* **270**, 678 (1983).
15. S. Rappaport, Ph. Podsiadlowski, P. C. Joss, R. Di Stefano, Z. Han, *Mon. Not. R. Astron. Soc.* **273**, 731 (1995).
16. T. M. Tauris, G. J. Savonije, *Astron. Astrophys.* **350**, 928 (1999).
17. Ph. Podsiadlowski, S. Rappaport, E. D. Pfahl, *Astrophys. J.* **565**, 1107 (2002).
18. The magnetospheric coupling parameter, $0.5 < \varphi < 1.4$ is a numerical factor of order unity depending on the accretion flow, the disk model, and the magnetic inclination angle of the pulsar (*10*, *11*, *32*–*34*).
19. S. L. Shapiro, S. A. Teukolsky, *Black Holes, White Dwarfs, and Neutron Stars: The Physics of Compact Objects* (Wiley-Interscience, New York, 1983).
20. S. A. Rappaport, J. M. Fregeau, H. C. Spruit, *Astrophys. J.* **606**, 436 (2004).
21. L. Burderi *et al.*, *Astrophys. J.* **560**, L71 (2001).
22. This "turn-off problem" has previously been debated elsewhere (*13*, *33*, *35*).
23. R. N. Manchester, J. H. Taylor, *Pulsars* (Freeman, San Francisco, CA, 1977).
24. D. R. Lorimer, A. G. Lyne, L. Festin, L. Nicastro, *Nature* **376**, 393 (1995).
25. F. Alberts, G. J. Savonije, E. P. J. van den Heuvel, O. R. Pols, *Nature* **380**, 676 (1996).
26. L. A. Nelson, E. Dubeau, K. A. MacCannell, *Astrophys. J.* **616**, 1124 (2004).
27. M. H. van Kerkwijk, C. G. Bassa, B. A. Jacoby, P. G. Jonker, in *Binary Radio Pulsars*, F. A. Rasio, I. H. Stairs, Eds. [Astronomical Society of the Pacific (ASP) Conference Series, San Francisco, CA, 2005], vol. 328, pp. 357–370.
28. This is the case if the pulsar spin period, $P$, is close to its initial spin period, $P_0$.
29. J. W. T. Hessels *et al.*, *Science* **311**, 1901 (2006).
30. L. Bildsten, *Astrophys. J.* **501**, L89 (1998).
31. D. Chakrabarty *et al.*, *Nature* **424**, 42 (2003).
32. Y.-M. Wang, *Astrophys. J.* **475**, L135 (1997).
33. F. Lamb, W. Yu, in *Binary Radio Pulsars*, F. A. Rasio, I. H. Stairs, Eds. (ASP Conference Series, San Francisco, CA, 2005), vol. 328, pp. 299–310.
34. C. R. D'Angelo, H. C. Spruit, *Mon. Not. R. Astron. Soc.* **406**, 1208 (2010).
35. M. Ruderman, J. Shaham, M. Tavani, D. Eichler, *Astrophys. J.* **343**, 292 (1989).
36. A. Patruno, *Astrophys. J.* **722**, 909 (2010).
37. I. S. Shklovskii, *Sov. Astron.* **13**, 562 (1970).


**Acknowledgments:** I gratefully thank N. Langer and M. Kramer for discussions and funding and without whom these results would not be possible and R. Eatough for helpful comments on the SOM. This work was partly supported by the Cluster of Excellence proposal EXC 1076, "The nature of forces and matter," at the University of Bonn. Radio pulsar data has been obtained from the *ATNF Pulsar Catalogue* (www.atnf.csiro.au/research/pulsar/psrcat/).

### Supporting Online Material

www.sciencemag.org/cgi/content/full/335/6068/561/DC1
Materials and Methods
SOM Text
Figs. S1 and S2
References (*38*–*54*)

8 November 2011; accepted 6 January 2012
10.1126/science.1216355

# Revealing the Superfluid Lambda Transition in the Universal Thermodynamics of a Unitary Fermi Gas

**Mark J. H. Ku, Ariel T. Sommer, Lawrence W. Cheuk, Martin W. Zwierlein***

**Fermi gases, collections of fermions such as neutrons and electrons, are found throughout nature, from solids to neutron stars. Interacting Fermi gases can form a superfluid or, for charged fermions, a superconductor. We have observed the superfluid phase transition in a strongly interacting Fermi gas by high-precision measurements of the local compressibility, density, and pressure. Our data completely determine the universal thermodynamics of these gases without any fit or external thermometer. The onset of superfluidity is observed in the compressibility, the chemical potential, the entropy, and the heat capacity, which displays a characteristic lambda-like feature at the critical temperature $T_c/T_F = 0.167(13)$. The ground-state energy is $\frac{3}{5}\xi N E_F$ with $\xi = 0.376(4)$. Our measurements provide a benchmark for many-body theories of strongly interacting fermions.**

Phase transitions are ubiquitous in nature: Water freezes into ice, electron spins suddenly align as materials turn into magnets, and metals become superconducting. Near the transitions, many systems exhibit critical behavior, reflected by singularities in thermodynamic quantities: The magnetic susceptibility diverges at a ferromagnetic transition, and the specific heat